

# A quasispecies on a moving oasis

Michael M. Desai\*, David R. Nelson

*Department of Physics, Jefferson Laboratories, Harvard University, 17 Oxford Street, Cambridge, MA 02138, USA*

Received 22 September 2003

Available online 8 December 2004

## Abstract

A population evolving in an inhomogeneous environment will adapt differently to different areas. We study the conditions under which such a population can maintain adaptations to a particular region when that region is not stationary, but can move. In particular, we consider a haploid population living near a moving favorable patch (“oasis”) in the middle of a large “desert.” At one genetic locus, individuals may have one of a few gene sequences that convey an advantage while in the oasis at the cost of a disadvantage in the desert. The distribution of genetic states in the population, possibly localized in genome space around the oasis-adapted genotypes, is known as a quasispecies. We find that the ratio of oasis-adapted individuals to desert-adapted ones exhibits sharp transitions at particular oasis velocities. We calculate an extinction velocity, and a switching velocity above which the dominance switches from the oasis-adapted genotype to the desert-adapted one. This switching velocity is analogous to the quasispecies mutational error threshold. Above this velocity, the population cannot maintain adaptations to the properties of the oasis.

© 2004 Elsevier Inc. All rights reserved.

*Keywords:* Quasispecies; Quasispecies transition; Extinction; Delocalization; Inhomogeneous environment

## 1. Introduction

Spatial inhomogeneities in the environment are often essential to understanding the dynamics of natural populations. Populations may for example be confined to limited reserves or live in an environment with gradients in resources or large-scale inhomogeneities in habitability. The evolution of a population in an inhomogeneous environment is particularly interesting. When individuals move over the environment sufficiently rapidly relative to the length scale of the inhomogeneities, they see and adapt to an “averaged” environment (Roughgarden, 1974; Wiens, 1976). When this is not true, however, the dynamics can be much more complex. Some individuals may randomly see primarily one part of the range while others see other parts. The population in the distant future will likely be

dominated by the descendants of a few exceptionally lucky individuals in the present, who will have seen an unusually favorable subset of the set of possible environments. Thus it is not at all clear a priori exactly how different regions of the environment will influence the evolution of the population.

This question of population genetics in a spatially non-uniform environment was first considered by Haldane (1948), who generalized the work of Fisher (1937) on the spread of a mutant in a uniform environment. He found that in environments where a particular allele is beneficial in one region and deleterious in another, its frequency will tend to be high in the regions where it is favored and low where it is disfavored, establishing a gene frequency “cline.” The properties of such a cline in one dimension in a diploid population experiencing migration, selection, and genetic drift have been analyzed by a number of authors (Endler, 1973; Felsenstein, 1975; Fisher, 1950; Nagylaki, 1975; Slatkin, 1973; Slatkin and Maruyama, 1975).

\*Corresponding author. Fax: +1 617 496 1541.

E-mail address: [desai@fas.harvard.edu](mailto:desai@fas.harvard.edu) (M.M. Desai).

More recent work has extended this analysis to consider multiple alleles at the selected locus in arbitrary spatial geometries (You and Nagylaki, 2002).

In this paper, we consider a simple environment with two regions, a favorable “oasis” in a large less favorable (or unfavorable) “desert,” as studied by several previous authors (Hanson, 1966; Nagylaki, 1975, 1978). The favorable area could be realized as a game reserve, a region of favorable climatic conditions, or a patch of light, among other things. Provided that the favorable region is stationary and sufficiently large, a population will adapt to the special properties of this region (Hanson, 1966; Nagylaki, 1975). Alleles with an advantage in each area will be more common there, and a steady-state gene frequency cline will become established. However, in many cases the oasis will move at some typical velocity  $v$ , for example due to seasonal weather patterns or human intervention. Equivalently, the population could be blown across the oasis at speed  $v$  by asymmetric migration (May et al., 1975; Nagylaki, 1978; Pauwelussen and Peletier, 1981) or some other form of “wind.” In this situation, there is a velocity beyond which the population will not be able to maintain adaptations to the properties of the oasis. Rather, the evolution will be dominated only by the desert environment. We focus in this paper on calculating this velocity, which we call the “switching velocity”.

We consider population densities  $\mathbf{c}(\vec{x}, t)$  given by a linearized Fisher equation with drift,

$$\frac{\partial \mathbf{c}(\vec{x}, t)}{\partial t} = D \nabla^2 \mathbf{c} - \vec{v} \cdot \nabla \mathbf{c} + \mathcal{R}(\vec{x}) \mathbf{c}, \quad (1)$$

where  $D$  is the diffusion constant and  $\vec{v}$  is the drift velocity. We consider a haploid population with two types of individuals. Thus  $\mathbf{c}(\vec{x}, t)$  is a two-vector

$$\mathbf{c}(\vec{x}, t) = \begin{pmatrix} c_1(\vec{x}, t) \\ c_2(\vec{x}, t) \end{pmatrix} \quad (2)$$

and  $\mathcal{R}(\vec{x})$  is a two-by-two matrix with diagonal elements specifying the growth rates of the two genotypes and off-diagonal elements specifying the mutation and back-mutation rates. A nonlinear saturation term can be added, and is important for some purposes. We assume that the population  $c_1$  has some gene or sequence which conveys an advantage in the oasis, but has an overall cost which makes it disadvantageous in the desert. The population  $c_2$  consists of all individuals who have lost the function of the gene by one or more mutations. Individuals of type 1 are thus those that have adapted to the special properties of the oasis, while type 2 individuals are desert-adapted.

This is a simplified model of a quasispecies, which is a distribution of genome sequences localized in sequence space around an “ideal” sequence. In our model,

genotype 1 represents the population of the “ideal” sequence, while type 2 represents all others. There is mutation back and forth between the two, typically with the mutation rate away from the ideal sequence greater than the mutation rate towards it. A few recent papers have examined other versions of a spatial quasispecies model, with many different possible types of individuals representing all possible Hamming distances from the ideal sequence (Altmeyer and McCaskill, 2001; Gerland and Hwa, 2002). Here, we focus on a simple two-type spatial model, although it is straightforward to generalize our results. Our model is qualitatively similar to that of Nagylaki (1978), though Nagylaki neglects mutation and considers a diploid population.

Our analysis is an extension of previous work examining a population without genetic structure diffusing and drifting in a random environment. Nelson and Shnerb (1998) examine such a population in two dimensions in the case where the population growth rate is a random function of  $\vec{x}$ , using the non-Hermitian methods developed by Hatano and Nelson (1997, 1998). In the limit of small  $v$  ( $v \ll v_F \equiv 2\sqrt{aD}$ , where  $a$  is the average of  $r(x)$ ), the population is dominated by a few colonies that grow up around “oases,” regions which happen to have higher growth rates than surrounding areas. As  $v$  increases, individual colonies on less prosperous oases are blown away in a series of “delocalization” transitions. In the limit of large  $v$  all organisms are blown away from individual oases and convect across the environment. At long times, the population is dominated by those individuals that happened to take very special paths through the random environment, travelling through a disproportionate number of the oases. Thus, this is an example of a system in which a typical individual will evolve in response to a very special subset of the environment. In subsequent work, Dahmen et al. (2002) examined the transition between the small and large  $v$  regimes by looking at a model of a single oasis. Their predictions have been qualitatively confirmed by recent experiments on *Bacillus subtilis* growth (Neicu et al., 2000).

We generalize the work of Dahmen et al. (2002) to consider the genetic state of our population as we change the velocity  $v$ . We find two important transitions. When the growth rate in the desert is negative, there is an extinction velocity  $v_e$  where the entire population goes extinct. When the genotype 2 desert growth rate is positive, there is a “switching” velocity  $v_s$  where the behavior of the population changes dramatically. Below this velocity the population (particularly within the oasis) is dominated by genotype 1. Above it, the oasis-adapted genotype is outcompeted, genotype 2 dominates, and  $c_1/c_2 \rightarrow 0$  at long times. This transition is a velocity-driven analog of the classical mutational error threshold in non-spatial quasispecies models (Eigen, 1971; Eigen et al., 1989; McCaskill, 1984).

Our results have interesting implications. If the oasis represents some part of a species' habitat, the switching velocity is simply how quickly this can move before the species can no longer maintain adaptations to the properties of this aspect of its range. Our analysis is also a first step towards understanding the spatial quasispecies model in a random environment, where the population does not evolve in response to the averaged environment but rather in response to a different, highly selective subset of the environment.

The outline of this paper is as follows. In Section 2, we give a detailed description of our model. In Section 3, we outline the calculation of the critical velocities and the behavior of the population in the different regimes. In Section 4, we compare our analytical results with computer simulations. Finally, in Section 5, we discuss the main biological implications of these calculations.

## 2. Model

We consider a population with two types of individuals whose densities are described by

$$\mathbf{c}(\vec{x}, t) = \begin{pmatrix} c_1(\vec{x}, t) \\ c_2(\vec{x}, t) \end{pmatrix}. \quad (3)$$

The dynamics is exponential growth (or decay) with diffusion and convection

$$\frac{\partial \mathbf{c}(\vec{x}, t)}{\partial t} = D \nabla^2 \mathbf{c} - \vec{v} \cdot \vec{\nabla} \mathbf{c} + \mathcal{R}(\vec{x}) \mathbf{c}, \quad (4)$$

where  $\mathcal{R}(\vec{x})$  is a two-by-two matrix. We are primarily concerned with the extinction and delocalization transitions. Thus for the bulk of our analysis, we neglect the possibility of a nonlinear saturation term. In Section 5.1 we discuss the consequences of such a nonlinearity.

We define the growth and death rates of individuals of type  $i$  within the oasis to be  $\alpha_i$  and  $\gamma_i$ , respectively. Outside the oasis, the growth and death rates are defined to be  $\beta_i$  and  $\delta_i$ . The probability that a type 1 mother will produce a type 2 daughter because of mutation is defined to be  $\mu_1$ , and the back-mutation probability is  $\mu_2$ . Based on these definitions, the matrix  $\mathcal{R}(\vec{x})$  is given by

$$\mathcal{R}(\vec{x}) = \begin{pmatrix} \alpha_1 - \gamma_1 - \mu_1 \alpha_1 & \mu_2 \alpha_2 \\ \mu_1 \alpha_1 & \alpha_2 - \gamma_2 - \mu_2 \alpha_2 \end{pmatrix} \quad (5)$$

inside the oasis and similarly (with  $\alpha \rightarrow \beta$  and  $\gamma \rightarrow \delta$ ) in the desert.

We next define the Malthusian parameters  $a_i \equiv \alpha_i - \gamma_i$  and  $b_i \equiv \beta_i - \delta_i$ . For simplicity, we assume that the growth rates within the desert and the oasis are the same, i.e.  $\alpha_i = \beta_i$ . This means that the desert is less hospitable because of a higher death rate, not a lower

growth rate. This yields the growth rate matrix

$$\mathcal{R}(\vec{x}) = \begin{pmatrix} a_1 - \mu_1 \alpha_1 & \mu_2 \alpha_2 \\ \mu_1 \alpha_1 & a_2 - \mu_2 \alpha_2 \end{pmatrix} \quad (\text{inside oasis}) \quad (6)$$

in the oasis and similarly in the desert,

$$\mathcal{R}(\vec{x}) = \begin{pmatrix} b_1 - \mu_1 \alpha_1 & \mu_2 \alpha_2 \\ \mu_1 \alpha_1 & b_2 - \mu_2 \alpha_2 \end{pmatrix} \quad (\text{outside oasis}). \quad (7)$$

The results for  $\alpha \neq \beta$  are also straightforward to calculate with our methods. However, the assumption  $\alpha_i = \beta_i$  simplifies the analysis by implying that the effective mutation rates per unit time inside and outside the oasis are the same. If mutation rates are constant per unit time rather than per generation, this is true anyway (in this case, we simply replace  $\mu_i \alpha_i \rightarrow \mu_i$  throughout). In our discussion, however, we retain the definition of  $\mu_1$  and  $\mu_2$  as mutation probabilities per generation.

We consider the case where any individual is better off in the oasis than the desert (i.e. it is a beneficial oasis), but genotype 1 holds a relative advantage in the oasis and genotype 2 holds a relative advantage in the desert. That is, genotype 1 is beneficial in one region (the oasis) and deleterious elsewhere, as in classical cline models. This implies  $a_1 > b_1$ ,  $a_2 > b_2$ ,  $a_1 > a_2$ , and  $b_2 > b_1$ . Absent these inequalities, one or the other type will be more fit everywhere, and this type will unequivocally dominate the population (up to the mutational error threshold), independent of the drift velocity. In that case, we can ignore the inferior type at long times and the problem reduces to that studied by Dahmen et al. (2002). Our assumptions imply that individuals of type 1 have some function that conveys an advantage inside the oasis, at the cost of a disadvantage elsewhere. Our analysis will determine whether or not this function can be maintained in the face of mutational pressure when the oasis is moving at velocity  $v$ .

We could of course make any number of assumptions about the geometry of the desert and the oasis. We consider for simplicity a one-dimensional system with an oasis of width  $W$  in the middle of an infinite desert, as depicted in Fig. 1a. This analysis also describes the long-time behavior of the two-dimensional system with geometry as described by Fig. 1b. If the initial conditions are uniform in the  $y$  direction, the one-dimensional system of Fig. 1a is equivalent to the two-dimensional system of Fig. 1b. If the conditions are non-uniform, the two become equivalent after a time of order  $\ell^2/D$  (Dahmen et al., 2002). More complex geometries are certainly possible, and we discuss these briefly in Section 5.2.

We assume throughout that differential equations are an adequate representation of these biological processes. We neglect genetic drift and discreteness in population number, which may have some importance near the extinction transition. The effects of discreteness may be

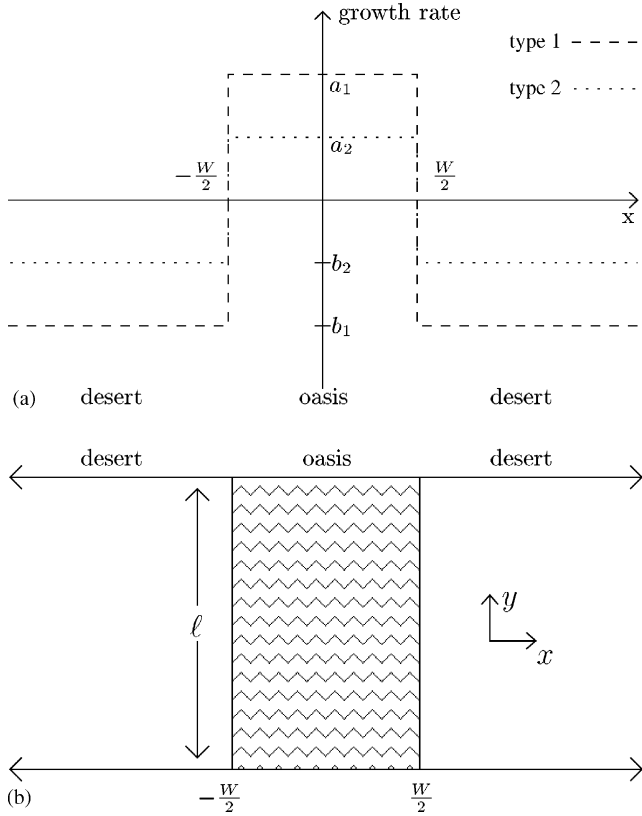


Fig. 1. (a) The one-dimensional system we consider, for the case of a deadly desert. The dashed line is the growth rate of genotype 1, the dotted line the growth rate of genotype 2. This is an approximation to the two-dimensional system shown in (b), valid when the initial conditions are uniform in the  $y$  direction or the time is greater than  $\ell^2/D$ .

analyzed using the methods of Doi (1976a, b), Peliti (1985), and Cardy and Tauber (1996).

### 3. Calculation of the population dynamics

We analyze our model using non-Hermitian methods (Hatano and Nelson, 1997, 1998; Nelson and Shnerb, 1998). We first rewrite our system in the form

$$\frac{\partial \mathbf{c}(x, t)}{\partial t} = \mathcal{L} \mathbf{c}, \quad (8)$$

where  $\mathcal{L}$  is given by  $\mathcal{L} = \mathcal{L}_{in} \theta(W/2 - |x|) + \mathcal{L}_{out} \theta(|x| - W/2)$ , and  $W$  is the width of the oasis. The function  $\theta(y) = 1$  if  $y \geq 0$  and 0 otherwise, and

$$\mathcal{L}_{in} = \begin{pmatrix} D\partial_x^2 - v\partial_x + a_1 - \mu_1\alpha_1 & \mu_2\alpha_2 \\ \mu_1\alpha_1 & D\partial_x^2 - v\partial_x + a_2 - \mu_2\alpha_2 \end{pmatrix}, \quad (9)$$

$$\mathcal{L}_{out} = \begin{pmatrix} D\partial_x^2 - v\partial_x + b_1 - \mu_1\alpha_1 & \mu_2\alpha_2 \\ \mu_1\alpha_1 & D\partial_x^2 - v\partial_x + b_2 - \mu_2\alpha_2 \end{pmatrix}. \quad (10)$$

$\mathcal{L}$  is non-Hermitian, but we can diagonalize it with a system of left and right eigenfunctions  $\phi_n^L(x)$  and  $\phi_n^R(x)$ , with their (common) eigenvalues  $\Gamma_n$ . These eigenfunctions (which we also call “states”) satisfy the orthonormality condition

$$\int \phi_m^L(x) \cdot \phi_n^R(x) dx = \delta_{mn}. \quad (11)$$

Using this result, we can write the initial condition as a linear superposition of the right eigenfunctions, i.e.  $\mathbf{c}(x, t = 0) = \sum_n c_n \phi_n^R(x)$ , where

$$c_n = \int d^d x \phi_n^L(x) \cdot \mathbf{c}(x, t = 0). \quad (12)$$

We can then immediately write down the solution valid for all times, namely

$$\mathbf{c}(x, t) = \sum_n c_n \phi_n^R(x) e^{\Gamma_n t}. \quad (13)$$

This result has a clear biological interpretation. Initially, the population is in some particular arrangement, expressible as a linear combination of the different eigenfunctions. Due to the structure of the eigenfunctions, this combination will necessarily include the eigenfunction corresponding to the largest  $\Gamma_n \equiv \Gamma_{gs}$  (which is always real). This eigenfunction is special, and we refer to it as the “ground state.” As time passes, the population distribution looks more and more like the ground state. This distribution will grow (or die out) exponentially with rate  $\Gamma_{gs}$ . The other  $\phi_m^R$  may be important initially, but since they grow more slowly than the ground state, they soon become irrelevant. Thus understanding the ground state function and its eigenvalue are the key to understanding the long time behavior of the population.

It remains to solve for the eigenfunctions and eigenvalues  $\phi_n^L(x)$ ,  $\phi_n^R(x)$ , and  $\Gamma_n$ . For the case  $v = 0$ , the solution is straightforward and will be discussed in detail below. For non-zero  $v$ , we make use of the fact that the eigenfunctions of  $\mathcal{L}_{v=0}$  are related to the eigenfunctions of  $\mathcal{L}$  by an “imaginary gauge transformation” (Nelson and Shnerb, 1998). That is, if  $\phi_{n,v=0}^R(x)$  is a right eigenfunction of  $\mathcal{L}_{v=0}$  with eigenvalue  $\Gamma_n$ , then

$$\phi_{n,v}^R(x) = e^{vx/2D} \phi_{n,v=0}^R(x) \quad (14)$$

is a right eigenfunction of  $\mathcal{L}$ , with eigenvalue

$$\Gamma_n^v = \Gamma_n^{v=0} - \frac{v^2}{4D}, \quad (15)$$

as can be verified by allowing  $\mathcal{L}$  to act on  $\phi_n^R$ . Similar expressions hold for  $\phi_{n,v}^L$ . The eigenvalues  $\Gamma_n^{v=0}$  are all real. Thus, eigenfunctions for  $v > 0$  are very similar to the eigenfunctions for  $v = 0$ . The genotype 1 versus genotype 2 composition of the states is not altered at all. The only change is that the wind causes a distortion of the population in the direction of the wind, and the

growth rates of the states shift downward “rigidly” (i.e. independent of  $n$ ) by an amount  $\frac{v^2}{4D}$ .

However, this procedure works only for small  $v$ . To see this, consider the behavior of the eigenfunctions as  $x \rightarrow \infty$ . We expect (and will soon verify) that the  $v = 0$  eigenfunctions far from the oasis decay exponentially,

$$\phi_{n,v=0} \sim e^{-\kappa_n|x|}. \quad (16)$$

Thus for  $v > 0$ ,

$$\phi_n^R \sim e^{vx/2D - \kappa_n|x|}. \quad (17)$$

When  $v < 2D\kappa_n$ , the eigenfunctions vanish at infinity, as they should. However, for  $v > 2D\kappa_n$ , this function blows up at infinity, which is unreasonable. The correct eigenfunctions have a different character when  $v > 2D\kappa_n \equiv v_n^*$ .

Hatano and Nelson (1998) show that the transition at  $v_n^*$  is a delocalization of the corresponding eigenfunction. For  $v < v_n^*$ , the eigenfunctions are localized around the oasis, but for  $v > v_n^*$  they are delocalized. This makes intuitive sense. For small velocities, the population will tend to cluster around the oasis, but for larger wind velocities it gets blown off the oasis and must live by drifting across the desert. The behavior of the eigenvalues  $\Gamma_n$  near this delocalization transition is striking. Up to  $v_n^*$ , the eigenvalue  $\Gamma_n^v$  is simply equal to  $\Gamma_n^{v=0} - \frac{v^2}{4D}$ , but beyond this point this relation no longer holds. Instead,  $\Gamma_n$  jumps off the real axis at  $v_n^*$ , becoming complex, and the eigenfunctions become broad delocalized states extending through the desert (Hatano and Nelson, 1997, 1998; Nelson and Shnerb, 1998). We denote the value of  $\Gamma_n$  at which this occurs by  $\Gamma_n^*$ . As we continue to increase  $v$  above  $v_n^*$ , the real part of  $\Gamma_n$  stays approximately constant, although the imaginary part does change. From the gauge transformation relationship, we have  $\Gamma_n^* = \Gamma_n^{v=0} - \frac{(v_n^*)^2}{4D}$ . However, as we will see, the structure of the  $n$ -dependence of  $v_n$  and  $\Gamma_n$  is such that there are only two different values of  $\Gamma_n^*$ . This is a crucial point. In our problem, the states will divide into those dominated by genotype 1 and those dominated by genotype 2. As we will show, states dominated by genotype 1 delocalize at  $\Gamma_1^* = \langle r_1 \rangle$ , the spatial average growth rate of the first genotype, which up to finite size effects is just  $b_1$ .  $\Gamma_2^* = \langle r_2 \rangle \approx b_2$  plays the same role for states dominated by the second genotype. By our assumptions about the parameters,  $\Gamma_2^* > \Gamma_1^*$ . An example of eigenvalue spectra for several values of  $v$  is given in Fig. 2.

Each localized state has some particular  $\Gamma_n^{v=0}$ , and for non-zero  $v$  its eigenvalue becomes  $\Gamma_n = \Gamma_n^{v=0} - \frac{v^2}{4D}$ . As  $v$  increases,  $\Gamma$  decreases until the state delocalizes, at  $\Gamma_1^*$  for those states dominated by type 1 and at  $\Gamma_2^*$  for those states dominated by type 2. We will see that the ground state for  $v = 0$  is dominated by genotype 1. As  $v$  increases there comes a critical point when this ground

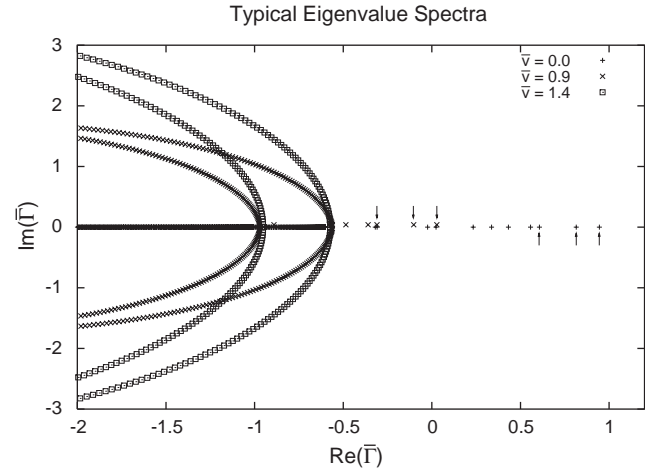


Fig. 2. An example of eigenvalue spectra, shown here for 3 values of  $\bar{v} = \frac{v}{v_F} \equiv \frac{v}{2\sqrt{Dq_1}}$  with  $\bar{a}_1 = \bar{a}_1 = 1, \bar{b}_1 = -1, \bar{a}_2 = \bar{a}_2 = 0.6, \bar{b}_2 = -0.6, \mu_1 = 0.01, \mu_2 = 0.001$ , and  $\bar{D} = 0.25$ , where the overbars indicate the non-dimensionalized parameters discussed in Appendix C. To allow easy distinction from the  $\bar{v} = 0$  results, the localized  $\bar{v} = 0.9$  eigenvalues have been shifted slightly upwards. Note the rigid shift of the localized eigenvalues (those on the real axis) to the left as we increase  $\bar{v}$ . This is highlighted by the three  $\bar{v} = 0$  states marked by upwards arrows, which for  $\bar{v} = 0.9$  are shifted into the three states marked by downwards arrows. The two (and only two) delocalization transitions  $\bar{\Gamma}_1^* \approx -1$  and  $\bar{\Gamma}_2^* \approx -0.6$  are also clearly visible. Note that these transition points, and all the delocalized states, do not shift to the left as  $\bar{v}$  increases. On the left half of the spectrum (omitted from the figure), the delocalized eigenstates form closed loops, an artifact of the computational discretization used to produce this figure.

state eigenvalue  $\Gamma_{gs}$  crosses  $\Gamma_2^*$ . Beyond this point it is no longer the ground state. Rather, the delocalized genotype-2 dominated state with eigenvalue  $\Gamma_2^*$  has the highest  $\Gamma$ , and this state determines the population dynamics. We call this critical velocity the “switching velocity,” where the dominance switches from genotypes 1 to 2. This switch is a type of quasispecies transition, caused not by exceeding a mutation rate error threshold, but by exceeding a critical velocity. This reasoning is illustrated in Fig. 3.

If the growth rate for genotype 2 in the desert is negative, then  $\Gamma_2^* < 0$ . The switching behavior will then be difficult to observe experimentally, as both genotypes will be going extinct when it happens. In this case, the biologically interesting transition occurs at the “extinction” velocity where the growth rate of the ground state passes through 0. Beyond this velocity, all the states have negative growth rate, so neither genotype can survive. When the growth rate for genotype 2 in the desert ( $b_2$ ) is positive, the switching velocity becomes biologically relevant. In this case, there is no extinction velocity. This is because the delocalized states do not shift to lower  $\Gamma$  as  $v$  increases, and at least one genotype-2 dominated delocalized state has eigenvalue  $\Gamma_2^* \approx b_2 > 0$ . Intuitively, this makes sense because the

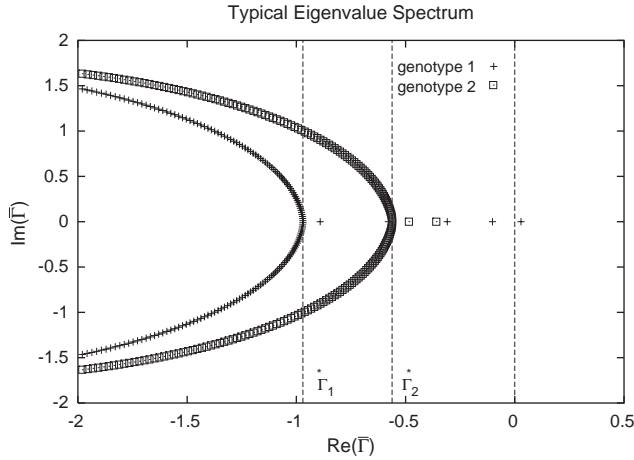


Fig. 3. A single eigenvalue spectrum, with the genotype-1 and genotype-2 dominated states distinguished. This is just the  $\bar{v} = 0.9$  spectrum from Fig. 2 above. Note the state with the largest  $\text{Re}(\Gamma)$  (i.e. the ground state) is a genotype-1 dominated state. This  $\bar{v}$  is just below the extinction velocity, so  $\Gamma_{gs}$  is just above the extinction threshold, indicated by the dashed vertical line at  $\Gamma = 0$ . As  $\bar{v}$  increases, all of the localized (real) states move to the left until they enter either the left parabola of delocalized states (for genotype-1 dominated states) or the right parabola of delocalized states (for genotype-2 dominated states). Thus as  $\bar{v}$  increases  $\Gamma_{gs}$  will soon pass through 0 at the “extinction velocity”. However, the delocalized states do not shift to the left as  $\bar{v}$  increases. Thus as  $\bar{v}$  increases further,  $\Gamma_{gs}$  will eventually pass through  $\Gamma_2^*$ , indicated by the center vertical line. Once this happens, the largest  $\text{Re}(\Gamma)$  no longer belongs to the original genotype-1 dominated state, but rather to a genotype-2 dominated delocalized state. The critical velocity at which this occurs is the “switching velocity.” In this example, since  $\Gamma_2^* < 0$ , the switching velocity is higher than the extinction velocity, and is therefore biological uninteresting. However, if we had  $\Gamma_2^* > 0$ , the spectrum would look identical, except it would be shifted to the right. We would then have  $\Gamma_2^* > 0$ , and hence there would always be states above  $\text{Re}(\Gamma) = 0$ . Thus there would be no extinction velocity, and the switching velocity would be biologically relevant.

population, dominated by genotype 2, can survive in the desert at arbitrarily large velocities.

### 3.1. Solution for the eigenvalues and eigenfunctions

In order to carry out the analysis sketched above, we must solve for the  $v = 0$  eigenvalues and eigenfunctions, and determine the values of  $\Gamma_1^*$  and  $\Gamma_2^*$ . It is possible to do this exactly, and an outline of this calculation is presented in Appendix A. However, it is more straightforward and instructive to first examine the solutions for  $\mu_1 = \mu_2 = 0$ , and then use perturbation theory to find the results for small  $\mu_1$  and  $\mu_2$ .

#### 3.1.1. The $\mu_1 = \mu_2 = 0$ solution

We first examine the system for  $\mu_1 = \mu_2 = 0$ . In this case, the two types of individuals are completely independent. The problem reduces to that studied by Dahmen et al. (2002). We use the imaginary gauge transformation to eliminate the velocity, and focus on

the  $v = 0$  eigenvalues and eigenstates. We then have to solve the eigenvalue equation

$$\mathcal{L}_{v=0} \phi_n^{i,v=0} = \Gamma_n^{i,v=0} \phi_n^{i,v=0}. \quad (18)$$

This problem is formally equivalent to the square well problem in quantum mechanics (Landau and Lifshitz, 1991). The  $v = 0$  right eigenstates are of the form

$$\phi_n^{1,v=0} = \begin{pmatrix} \psi_n^1 \\ 0 \end{pmatrix}, \quad \phi_n^{2,v=0} = \begin{pmatrix} 0 \\ \psi_n^2 \end{pmatrix}, \quad (19)$$

where

$$\psi_n^i = \begin{cases} A_n^i e^{\kappa_n^i x} & \text{for } x < -W/2, \\ B_n^i e^{ik_n^i x} + C_n^i e^{-ik_n^i x} & \text{for } -W/2 < x < W/2, \\ G_n^i e^{-\kappa_n^i x} & \text{for } x > W/2. \end{cases} \quad (20)$$

Note that the index  $i$  indicates the genotype that dominates the state. Substituting this ansatz into the eigenvalue equation leads to

$$\Gamma_n^{i,v=0} = D(\kappa_n^i)^2 + b_i = -D(k_n^i)^2 + a_i. \quad (21)$$

We proceed by requiring that  $\phi$  and its first derivative be continuous at  $x = \pm W/2$ , which determines the constants  $A, B, C$ , and  $G$  up to an overall normalization and yields a transcendental equation to determine  $\Gamma$ . This analysis is carried out in detail by Dahmen et al. (2002). The essential result is that provided the oasis is wide enough that a typical individual gives birth many times while diffusing across it, the ground state eigenvalue can be approximated as  $\Gamma_{gs}^{v=0, \mu=0} \approx a_1$ , with a corresponding eigenfunction that is entirely genotype 1 and localized largely within the oasis. We will use this approximation throughout the rest of this paper. We can also calculate the position of the delocalization transitions  $\Gamma_n^{i*}$ . These are defined as the amount by which the  $v = 0$  eigenvalue  $\Gamma_n^{i,v=0}$  is shifted by the delocalization velocity  $v_n^{i*}$ . We thus have  $\Gamma_n^{i*} = \Gamma_n^{i,v=0} - \frac{(v_n^{i*})^2}{4D} = \Gamma_n^{i,v=0} - D(\kappa_n^i)^2$ . Using Eq. (21), we find  $\Gamma_n^{i*} = b_i$ . Note that, as claimed above, this  $\Gamma_n^{i*}$  is independent of  $n$  and depends only on  $i$ . Thus there are two and only two delocalization thresholds, one corresponding to each genotype.

#### 3.1.2. Perturbation theory in $\mu_1$ and $\mu_2$

We can now examine the results for non-zero mutation rates  $\mu_1, \mu_2 > 0$  by using a non-Hermitian version of time-independent perturbation theory from quantum mechanics (Landau and Lifshitz, 1991). We require that  $\mu_1$  and  $\mu_2$  be small, specifically that  $\frac{\mu_1 \alpha_i}{a_1 - a_2}, \frac{\mu_2 \alpha_i}{b_2 - b_1} \ll 1$ . The details of the calculation are described in Appendix B. The eigenstates now all involve both genotypes, although those that began as genotype 1 states remain dominated by this type, and

vice versa. More precisely, we have

$$\phi_n^{1,v=0,R} = \begin{pmatrix} \psi_n^1 \\ \frac{\mu_1 \alpha_1}{a_1 - a_2} \psi_n^2 \end{pmatrix} \quad (22)$$

for a genotype-1 dominated localized state, and

$$\phi_n^{2,v=0,R} = \begin{pmatrix} \frac{\mu_2 \alpha_2}{b_2 - b_1} \psi_n^1 \\ \psi_n^2 \end{pmatrix} \quad (23)$$

for a genotype-2 dominated delocalized state, where  $\psi_n^1$  and  $\psi_n^2$  are given in Section 3.1.1. Note that we focus on genotype-1 dominated localized states and genotype-2 dominated delocalized states because no other state can dominate the dynamics in any regime. The eigenvalues are also shifted. The eigenvalues for genotype-1 dominated localized states become

$$\Gamma_n^{1,v=0} = \Gamma_n^{i,v=0,\mu=0} - \mu_1 \alpha_1 + \frac{\mu_1 \alpha_1 \mu_2 \alpha_2}{a_1 - a_2}, \quad (24)$$

while the genotype-2 dominated delocalized states have eigenvalues

$$\Gamma_n^{2,v=0} = \Gamma_n^{2,v=0,\mu=0} - \mu_2 \alpha_2 + \frac{\mu_1 \alpha_1 \mu_2 \alpha_2}{b_2 - b_1}, \quad (25)$$

plus higher-order terms in  $\mu_1$  and  $\mu_2$ .

### 3.2. Critical velocities

We can now calculate the critical velocities at which the dynamics changes qualitatively. There are two relevant cases. For  $b_2 < 0$  neither delocalization transition occurs at positive  $\Gamma$  because neither genotype can survive in the desert. Thus the switching velocity, though it exists formally, is biologically irrelevant. The extinction velocity  $v_e$  is the velocity where the ground state eigenvalue passes through zero. Below  $v_e$  a genotype-1 dominated population can multiply but above this velocity the population must go extinct. This velocity is defined by  $\Gamma_{gs}^{v_e} = \Gamma_{gs}^{v=0} - \frac{v_e^2}{4D} = 0$ , which using Eq. (24) gives

$$v_e = 2\sqrt{Da_1} \left[ 1 - \frac{\mu_1 \alpha_1}{2a_1} \right], \quad (26)$$

valid to first order in  $\mu_1$  and  $\mu_2$ . Note that for  $\mu_1 = 0$ , we have  $v_e = v_F \equiv 2\sqrt{Da_1}$ , the Fisher velocity for genotype 1.

For  $b_2 > 0$  there is no extinction velocity, as genotype 2 can survive at any velocity. However, there is a switching velocity  $v_s$  where the population shifts from being mostly genotype 1 to mostly genotype 2. This occurs when the growth rate of the genotype-1 dominated ground state passes through  $\Gamma_2^* = b_2 - \mu_2 \alpha_2 + \frac{(\mu_2 \alpha_2)^2}{b_2 - b_1}$ . By a similar calculation we find

$$v_s = 2\sqrt{D(a_1 - b_2)} \left[ 1 - \frac{1}{2} \frac{\mu_1 \alpha_1}{a_1 - b_2} + \frac{1}{2} \frac{\mu_2 \alpha_2}{a_1 - b_2} \right], \quad (27)$$

also valid to first order in  $\mu_1$  and  $\mu_2$ . As mentioned above, this switching velocity is a sort of quasispecies transition. As the velocity increases past this critical threshold, the population can no longer maintain the “ideal” sequence, even if it is below the mutational error threshold. This switching velocity is also well defined for  $b_2 < 0$ , but will be difficult to observe because  $v_s > v_e$ . We can easily calculate the second-order corrections to both  $v_e$  and  $v_s$  (see Appendix B).

## 4. Simulations

We use two different computational methods to test our analytic results. First, we use a lattice discretization of the Liouville operator  $\mathcal{L}$  to calculate the eigenvalue and eigenfunction spectrum for particular sets of parameter values. This numerical work provides an aid to intuition and one check of the validity of our approximations. Second, we simulate the underlying discrete process, namely individuals multiplying and mutating at appropriate rates. This tests not just the results of our analysis, but also the overall applicability of continuous time differential equations to the real discrete populations we model.

### 4.1. Lattice approximation to the Liouville operator

We made several approximations in arriving at our analytical results, including an approximation for  $\Gamma_{gs}$  and for the shifts in eigenvalues with  $\mu_1$  and  $\mu_2$ . To test these approximations, we calculate the eigenvalue spectrum numerically. We discretize space, find the resulting discretized Liouville operator, and numerically diagonalize it for a particular set of parameters. The details of this method are described in Appendix C.

This approach allows us to determine the shifts in the growth rates as  $\mu$  or  $v$  is varied, and hence the critical velocities  $v_e$  and  $v_s$ . We can compare these results to our analytical predictions, and therefore confirm our calculation of the critical velocities. This comparison for one particular set of parameters is shown in Fig. 4. Comparisons for other parameter values have been carried out, and give similar results. The eigenvalue spectra shown in Figs. 2 and 3 were also obtained in this way.

### 4.2. Simulations of the discrete system

We can also simulate the underlying discrete process which inspired our formulation of the differential equations we analyze in this paper. We discretize space, placing individuals on a one-dimensional lattice which represents our environment. These individuals move around, proliferate, die, and mutate. We also impose a saturation term so that at long times the population distribution settles down to a steady state.

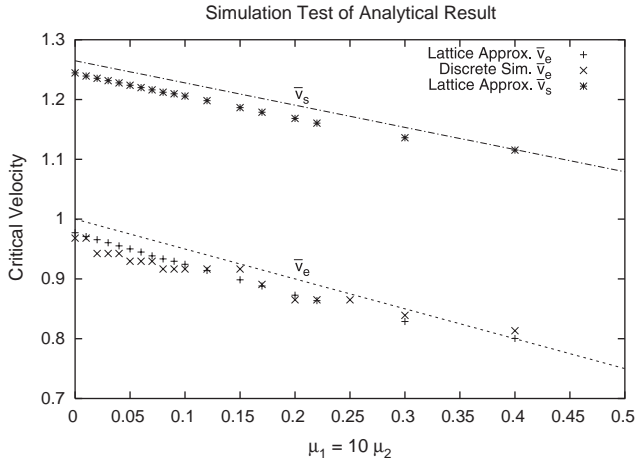


Fig. 4. A comparison of the critical velocities  $\bar{v}_e$  and  $\bar{v}_s$  between the simulations and the analytical result, as a function of  $\mu_1 = 10\mu_2$ . The analytical result is shown as a dashed line for  $\bar{v}_s$  and a dotted line for  $\bar{v}_e$ . Here we have  $\bar{a}_1 = \bar{\alpha}_1 = 1$ ,  $\bar{a}_2 = \bar{\alpha}_2 = 0.6$ ,  $\bar{b}_1 = -1$ ,  $\bar{b}_2 = -0.6$ , and  $\bar{D} = 0.25$ , where the overbars indicate the dimensionless units described in Appendix C. This result is typical of such comparisons for other parameter values. For these parameters, we expect the perturbation calculation of the analytical result to be valid for  $\mu_1 \ll 0.4$ . The slight overestimates of  $\bar{v}_e$  and  $\bar{v}_s$  by the analytic theory for small  $\mu_1$  are due to finite size effects. The underestimate as  $\mu_1$  grows beyond the range of our perturbation expansion is due to the importance of higher-order terms.

By comparing the steady-state population profiles for different values of  $v$ , we determine  $v_e$  or  $v_s$ . These results can then be compared to the analytical results. This comparison, for one particular set of parameters, is shown in Fig. 4. Note that this comparison is only for  $v_e$ , as for these parameter values  $v_s$  is not biologically relevant and is thus impossible to observe with this type of simulation. The details of this method are described in Appendix D.

5. Discussion

To interpret our results, it is helpful to first consider the behavior of a non-spatial quasispecies model. We imagine a population living in a uniform environment whose conditions match those of the oasis. Genotype 1 grows more quickly, but there is a mutational pressure away from this “ideal” genotype. Mutation away from this sequence is typically expected to be much more frequent than mutation back, so it is common in such models to set  $\mu_2 = 0$ . It is then straightforward to calculate the composition of the population. We find that the equilibrium ratio of genotypes 1 to 2 individuals  $q$  ( $q \equiv c_1/c_2$ ) is given by

$$q = \frac{a_1 - a_2 - \mu_1 \alpha_1}{\mu_1 \alpha_1}. \tag{28}$$

Thus, the ratio of species 1 to 2 decreases with increasing  $\mu_1$  until  $\mu_1$  reaches the critical “error threshold” for this quasispecies model. At this threshold,  $\mu_1^c = \frac{a_1 - a_2}{\alpha_1}$ , the “ideal” genotype can no longer survive and the population becomes completely dominated by genotype 2. This is the most famous result of Eigen’s quasispecies model (Eigen, 1971; Eigen et al., 1989; McCaskill, 1984).

Our analysis finds that, in analogy to the quasispecies error threshold, in the spatial model there is a velocity threshold above which genotype 1 is outcompeted by genotype 2. This velocity, which we call the switching velocity  $v_s$ , is given by Eq. (27). If the growth rate of genotype 2 in the desert is positive, we can expect to see this behavior in a real system. Our model naturally also has the traditional error threshold; for  $\mu_1 > \frac{a_1 - a_2}{\alpha_1}$  and  $\mu_2 = 0$ , genotype 1 is outcompeted by genotype 2 regardless of  $v$ . It would be interesting to explore the interactions between the mutation-driven and velocity-driven quasispecies transitions. However, our analysis is based on the assumption of small mutation rates and thus focuses on the velocity-driven transition under the assumption that we are well away from the mutation-driven transition (although it would be possible in principle to use the exact solution discussed in Appendix A to explore the velocity-driven transition near the mutational threshold). A qualitative phase diagram of the different velocity-driven transitions is given in Fig. 5.

Our model describes a number of important biological situations. The oasis could be a particularly favorable patch of the environment or a zone of favorable climatic conditions which is moving at a typical speed  $v$  due to seasonal weather patterns or shifts in climate. A population can take advantage of this oasis by adapting to these conditions, but then will fare worse in the rest of the space. Our analysis explores how fast the oasis can move before the population can no longer

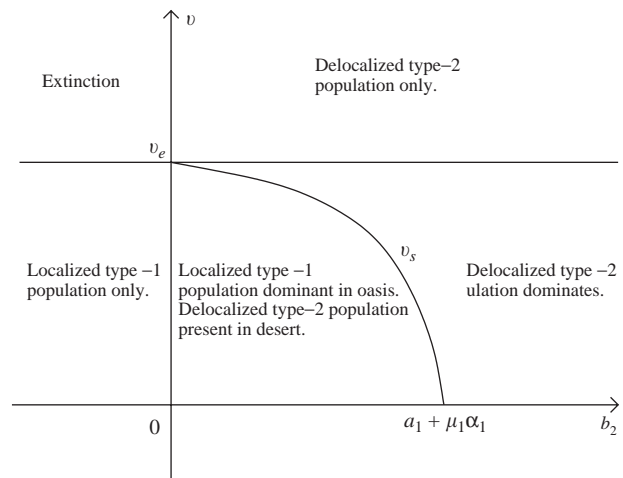


Fig. 5. A phase diagram showing the transitions as a function of  $v$  and  $b_2$ . This figure accounts for the qualitative effects of a nonlinear saturation term.

maintain an adaptation to the favorable patch. Beyond this speed individuals may occasionally find themselves in the oasis but cannot adapt quickly enough to benefit.

Throughout our analysis, we assume that the environment has no explicit time dependence. Non-spatial populations in time-dependent environments have also been the subject of much recent work (Burger and Lynch, 1995; Nilsson and Snoad, 2002; Wilke and Ronnewinkel, 2001; Wilke et al., 2001). In such a system, if the mutation rate is too low compared to the rate of change of the environment, the population cannot “track” the changing optimal genotype (Kamp and Bornholdt, 2002; Nilsson and Snoad, 2000). This is another quasispecies transition, analogous to the velocity-driven threshold that we analyze. Below the mutational threshold the population cannot maintain an adaptation to the moving fitness peak in genotype space, while above the velocity threshold the population cannot adapt to the moving oasis in real space. The dynamics in genome space and real space can be quite different, but the interactions between the two in a time-dependent spatial environment is an interesting area for future work.

Besides showing the existence of the velocity-driven quasispecies transition, our results make 5 interesting biological predictions. We discuss each of these in turn.

(1) *The overall population growth rate decreases as  $v^2$  up to the critical velocity:* The imaginary gauge transformation tells us that for  $b_2 < 0$ , the exponential growth rate of the population decreases as  $\frac{v^2}{4D}$  until it goes extinct at  $v_e = 2\sqrt{a_1 D} \left(1 - \frac{\mu_1 \alpha_1}{2a_1}\right)$ . For  $b_2 > 0$  the exponential growth rate of the population decreases again by  $\frac{v^2}{4D}$  until it reaches  $v_s = 2\sqrt{(a_1 - b_2)D} \left(1 - \frac{\mu_1 \alpha_1}{a_1 - b_2} + \frac{\mu_2 \alpha_2}{a_1 - b_2}\right)$ . Increasing the velocity further does not change the overall growth rate because a delocalized genotype 2 population then dominates.

(2) *Below the critical velocity, the genotype-1 dominated population will extend somewhat into the desert:* The type-1 population will extend a typical distance  $\xi = \frac{1}{\kappa_{gs} - \frac{v}{2D}}$  into the desert. From the relationship between  $\kappa$  and  $\Gamma$  we find that this typical distance is

$$\xi = \frac{2D}{2\sqrt{D(a_1 - b_1)} - v}, \quad (29)$$

independent of the mutation rates. Note that this diverges as  $(v_c - v)^{-1}$  as  $v \rightarrow v_c$  from below, where  $v_c \equiv 2\sqrt{D(a_1 - b_1)}$  is the velocity at which the type-1 dominated ground state eigenvalue  $\Gamma_{gs}$  reaches its delocalization threshold  $\Gamma_1^*$ . This divergence will be difficult to observe in real biological systems because  $v_s < v_c$ . Note for  $v \rightarrow 0$ ,  $\xi$  reduces to the classical result for the width of a cline (Slatkin, 1973), as we would expect.

(3) *The ratio of the two genotypes is proportional to  $\mu$ :* Below the switching velocity, the ratio of the number of type 2 individuals to type 1 in the oasis approaches  $\frac{\mu_1 \alpha_1}{a_1 - a_2}$  at long times. Above the switching velocity, the ratio of type 1 to 2 is  $\frac{\mu_2 \alpha_2}{b_2 - b_1}$  at long times. This result, however, is only true within the linear model. If we add a saturation term to the dynamics, this term will affect the long-time population ratios.

(4) *The ratio of genotype 1 to 2 is independent of  $v$  except when crossing  $v_s$ :* We might naively expect that as we increase  $v$ , the population gets driven more towards the desert, and thus the population shifts away from genotype 1 towards genotype 2. The gauge transformation ensures that this does not happen. Until we cross  $v_s$ , the ratio of genotypes in the ground state eigenfunction, and thus the population, remains constant. At  $v_s$  there is a sharp transition and the ratio of the genotypes shifts radically in favor of genotype 2. As we continue to increase the velocity, the ratio again remains constant. This result, however, is also only true within the linear model. A nonlinear saturation term “softens” the transition at  $v_s$ , as described in Section 5.1.

(5) *The “right” ratio of genotypes dominates exponentially:* If the initial state of the population below the switching velocity is all type 2, then type 1 will take over exponentially with a rate equal to the difference between  $\Gamma_{gs}$  and the dominant type 2 eigenvalue. This rate is just  $a_1 - a_2 - \mu_1 \alpha_1 + \mu_2 \alpha_2$ , and is independent of  $v$ . Similarly, if we begin with a type-1 dominated population above the switching velocity, the population will become dominated by genotype 2 exponentially with rate  $b_2 - b_1 - \mu_2 \alpha_2 + \mu_1 \alpha_1$ , again independent of  $v$ .

### 5.1. Effects of a nonlinearity

Thus far we have concentrated on purely linear systems, without much discussion of nonlinear terms which cause the population to saturate. This approximation is justified because the presence of a nonlinear saturation term will not affect the critical velocities. However, since all populations can be expected to saturate at some point, it is important to consider the general implications of such a nonlinearity.

In the discussion to this point, we have assumed that the eigenfunction with the largest growth rate will dominate the population, so that at long times we can neglect all but this dominant state. In the nonlinear case this is still roughly true. We can account for the effects of the nonlinearity by using mode couplings as in (Nelson and Shnerb, 1998), and anticipate that the fastest growing eigenfunction will suppress the others and dominate the population. There is, however, one important exception to this idea. For the problem considered here, the fastest-growing localized eigenfunction vanishes exponentially outside of the oasis, and hence will not suppress the growth of the

fastest-growing delocalized eigenfunction. Thus below the switching velocity  $v_s$ , the population is not in fact completely dominated by genotype 1. Rather, there is a genotype-1 dominated population inside the oasis and a genotype-2 dominated delocalized population in the desert. As we increase  $v$  we decrease the growth rate of the localized type 1 dominated state without changing the growth rate of the delocalized genotype-2 dominated state. Since the overall population sizes are set by the growth rates and the nonlinear terms, this will lead to a shift in the overall population density from type 1 to 2. Thus there will be some  $v$ -dependence in the genotype ratio even below  $v_s$ . Just above  $v_s$ , the fastest-growing delocalized eigenfunction will not completely suppress the fastest-growing localized eigenfunction, so similarly there will be some  $v$ -dependence above  $v_s$ . The transition at  $v_s$  is thus softened by the presence of the nonlinearity. While the dominance will still shift at this critical velocity, the transition will have some width dependent on the saturation term.

The nonlinearity will also impose a maximum carrying capacity on the system. As the system

$$\phi^R = \begin{cases} \begin{pmatrix} Ae^{-\kappa_1 x} + Be^{-\kappa_2 x} \\ Ce^{-\kappa_1 x} + Ee^{-\kappa_2 x} \end{pmatrix} & \text{for } \frac{W}{2} < x, \\ \begin{pmatrix} F \cos(k_1 x) + G \sin(k_1 x) + H \cos(k_2 x) + I \sin(k_2 x) \\ J \cos(k_1 x) + K \sin(k_1 x) + L \cos(k_2 x) + M \sin(k_2 x) \end{pmatrix} & \text{for } -\frac{W}{2} < x < \frac{W}{2}, \\ \begin{pmatrix} Ne^{\kappa_1 x} + Oe^{\kappa_2 x} \\ Pe^{\kappa_1 x} + Qe^{\kappa_2 x} \end{pmatrix} & \text{for } x < -\frac{W}{2}, \end{cases} \quad (30)$$

approaches this carrying capacity, the growth rates will slow down. Thus, if we start with an initial condition involving a population already near its carrying capacity, our analysis of the rate at which the “right” genotype composition is established will be an overestimate. While the results regarding the switching and extinction velocities and genotype composition still hold, the dynamics of reaching the resulting steady states will be slower. Our results for the rates are based on the linearization of the nonlinear model around  $c_1 = c_2 = 0$ , and so are valid as long as the ratio of the population to the carrying capacity is small compared to 1.

## 5.2. Other geometries

Many alternative geometries are clearly possible. One obvious choice is a circular oasis in an infinite desert, as considered by Dahmen et al. (2002). The primary effect of a non-trivial two-dimensional geometry is to change the eigenvalue spectrum. In particular,  $\Gamma_{gs}$  and, if the desert is not infinite,  $\Gamma_2^*$  will shift. The resulting change in the switching and extinction velocities will depend on the

growth rates  $a_i$  and  $b_i$  and the linear size of the oasis  $W$ , but not on  $\mu$ . However, the qualitative behavior is unaffected. Furthermore, if  $W$  is large compared to  $\sqrt{D/a}$ , the typical length an individual diffuses before giving birth (the precise requirement will vary with the specific geometry), this shift in critical velocities will vanish and the results will reduce to those calculated above.

## Acknowledgements

This work was supported in part by the National Science Foundation through Grant DMR-0231631, and through the Harvard Materials Science and Engineering Center through Grant DMR-0213805.

## Appendix A. Exact solution for the $v = 0$ system

It is straightforward, though tedious, to find the exact solution for the  $v = 0$  eigenfunctions and eigenvalues. We start with the ansatz

where the 16 parameters  $A, B, C, E, F, G, H, I, J, K, L, M, N, O, S, P$ , and  $Q$  are constant coefficients. Demanding that this ansatz satisfy the eigenvalue equation yields a system of 12 equations relating these constant coefficients,  $\kappa, k$ , and the eigenvalue  $\Gamma$ . We use 8 of these equations to eliminate 8 of the 16 coefficients, and the remaining 4 to determine  $\kappa_1, \kappa_2, k_1$ , and  $k_2$  in terms of the eigenvalue  $\Gamma$ . For small  $\mu_1$  and  $\mu_2$  ( $\frac{\mu_1 \mu_2 \alpha_1 \alpha_2}{(a_1 - a_2)^2} \ll 1, \frac{\mu_1 \mu_2 \alpha_1 \alpha_2}{(b_1 - b_2)^2} \ll 1$ ), we find

$$D\kappa_1^2 = \Gamma - b_2 + \mu_2 \alpha_2 + \frac{\mu_1 \alpha_1 \mu_2 \alpha_2}{b_2 - b_1}, \quad (31)$$

$$D\kappa_2^2 = \Gamma - b_1 + \mu_1 \alpha_1 - \frac{\mu_1 \alpha_1 \mu_2 \alpha_2}{b_2 - b_1}, \quad (32)$$

$$Dk_1^2 = -\Gamma + a_1 - \mu_1 \alpha_1 + \frac{\mu_1 \alpha_1 \mu_2 \alpha_2}{a_1 - a_2}, \quad (33)$$

$$Dk_2^2 = -\Gamma + a_2 - \mu_2 \alpha_2 - \frac{\mu_1 \alpha_1 \mu_2 \alpha_2}{a_1 - a_2}, \quad (34)$$

which serves to confirm our perturbation theory calculation. The expressions when  $\mu_1$  and  $\mu_2$  are not small are straightforward to calculate but unwieldy to write down.

We now demand that  $\phi$  and  $\frac{d\phi}{dx}$  be continuous at  $x = \pm \frac{W}{2}$ , yielding 8 equations for the remaining 9 unknowns (8 constant coefficients and  $\Gamma$ ). These results lead to a transcendental equation for  $\Gamma$ , the solutions to which are the eigenvalues of the system. Choosing a particular eigenvalue from among these possible solutions, we can easily determine the remaining unknowns (up to an overall normalization) from the rest of the equations. By requiring

$$\int \phi^L(x) \cdot \phi^R(x) dx = 1, \quad (35)$$

we determine the normalization, and thus the exact solution.

In practice, the transcendental equation for  $\Gamma$  is quite complicated and we can only solve it numerically. However, this exact approach does provide a useful check to the discretized numerical solution described in Section 4. The most important result is the  $\mu = 0$  ground state eigenvalue  $\Gamma_{gs}^{\mu=v=0}$ . Provided that the oasis is much wider than the distance a typical individual diffuses before giving birth, we have  $\Gamma_{gs}^{\mu=v=0} \approx a_1$  (Dahmen et al., 2002).

## Appendix B. Perturbation theory in $\mu_1$ and $\mu_2$

We can use standard perturbation theory from quantum mechanics to determine the results for  $\mu_1, \mu_2 > 0$  from the  $\mu_1 = \mu_2 = 0$  solution. We first rewrite the Liouville operator as  $\mathcal{L}_{v=0} = \mathcal{L}_0 + \mathcal{L}_1$ , where  $\mathcal{L}_1$  is proportional to the (small) mutation rates  $\mu_1$  and  $\mu_2$ , and

$$\mathcal{L}_0 = \begin{pmatrix} D\partial_x^2 + r_1(x) & 0 \\ 0 & D\partial_x^2 + r_2(x) \end{pmatrix},$$

$$\mathcal{L}_1 = \begin{pmatrix} -\mu_1\alpha_1 & \mu_2\alpha_2 \\ \mu_1\alpha_1 & -\mu_2\alpha_2 \end{pmatrix}, \quad (36)$$

where  $r_i(x) = (a_i + \mu_i\alpha_i)\theta(W/2 - |x|) + (b_i + \mu_i\alpha_i)\theta(|x| - W/2)$ . We know the eigenvalues and eigenfunctions of  $\mathcal{L}_0$  from Section 3. For our purposes, all that is necessary is that the eigenfunctions are an orthonormal set of left and right functions  $\phi_n^L$  and  $\phi_n^R$ .

From non-degenerate time-independent perturbation theory we find that the  $\mu > 0$  eigenvalues are related to the  $\mu = 0$  eigenvalues by the formula

$$\Gamma_n = \Gamma_n^{\mu=0} + \int \phi_n^L(x) \mathcal{L}_1 \phi_n^R(x) dx + \sum_{m \neq n} \frac{(\int \phi_m^L(x) \mathcal{L}_1 \phi_n^R(x) dx) (\int \phi_n^L(x) \mathcal{L}_1 \phi_m^R(x) dx)}{\Gamma_n^{\mu=0} - \Gamma_m^{\mu=0}}, \quad (37)$$

plus terms of third and higher order in  $\mathcal{L}_1$  (Landau and Lifshitz, 1991). Note that this result differs slightly from

standard theory because  $\mathcal{L}_1$  is non-Hermitian. The first-order term in  $\mathcal{L}$  is straightforward to calculate. It is simply  $-\mu_i\alpha_i$  for states dominated by genotype  $i$ . The second-order term is more complicated, because the  $\mu = 0$  eigenfunctions are of the form

$$\phi_n^R = \begin{pmatrix} \psi_n^1 \\ 0 \end{pmatrix} \quad \text{or} \quad \phi_n^R = \begin{pmatrix} 0 \\ \psi_n^2 \end{pmatrix}, \quad (38)$$

where the  $\{\psi_n^1\}$  and  $\{\psi_n^2\}$  each form an orthonormal set of eigenfunctions of the one-genotype problem. The  $\psi_n^1$  and  $\psi_n^2$  are almost, but not quite, orthonormal to each other.

In the approximation that these two sets of eigenfunctions are indeed orthonormal, the second order term for  $\Gamma_n$  is easy to calculate. For genotype-1 dominated localized states, it is  $\frac{\mu_1\alpha_1\mu_2\alpha_2}{a_1 - a_2}$ . For genotype-2 dominated delocalized states, it is  $\frac{\mu_1\alpha_1\mu_2\alpha_2}{b_2 - b_1}$ . In the same approximation, the corrections to the eigenfunctions are given by

$$\phi_n^{1,v=0,R} = \begin{pmatrix} \psi_n^1 \\ \frac{\mu_1\alpha_1}{a_1 - a_2} \psi_n^2 \end{pmatrix} \quad (39)$$

for a genotype-1 dominated localized state, and

$$\phi_n^{2,v=0,R} = \begin{pmatrix} \frac{\mu_2\alpha_2}{b_2 - b_1} \psi_n^1 \\ \psi_n^2 \end{pmatrix} \quad (40)$$

for a genotype-2 dominated delocalized state.

These results, and the observation that  $\Gamma_{gs}^{\mu=v=0} = a_1$  and  $\Gamma_{2,*}^{\mu=v=0} = b_2$ , allow us to calculate the critical velocities. To second order in  $\mu_1$  and  $\mu_2$ , the extinction velocity is given by

$$v_e = 2\sqrt{Da_1} \left[ 1 - \frac{\mu_1\alpha_1}{2a_1} - \frac{\mu_1^2\alpha_1^2}{8a_1^2} + \frac{\mu_1\mu_2\alpha_1\alpha_2}{2a_1(a_1 - a_2)} \right] \quad (41)$$

and the switching velocity is

$$v_s = 2\sqrt{D(a_1 - b_2)} \times \left[ 1 - \frac{\mu_1\alpha_1 - \mu_2\alpha_2}{2(a_1 - b_2)} - \frac{(\mu_1\alpha_1 - \mu_2\alpha_2)^2}{8(a_1 - b_2)^2} + \frac{\mu_1\alpha_1\mu_2\alpha_2}{2(a_1 - a_2)(a_1 - b_2)} - \frac{\mu_1\alpha_1\mu_2\alpha_2}{2(b_2 - b_1)(a_1 - b_2)} \right]. \quad (42)$$

The first order part of this result is quoted in Section 3 above.

This perturbation expansion relies on the assumption that  $\mu_1$  and  $\mu_2$  are small. Specifically, we require

$$\frac{\mu_i\alpha_i}{a_2 - a_1} \ll 1, \quad \frac{\mu_i\alpha_i}{b_2 - b_1} \ll 1 \quad (43)$$

for  $i = 1, 2$  for all of these results to be valid.

### Appendix C. Lattice approximation

Here we describe the details of the lattice approximation to the Liouville operator. We begin by discretizing space, replacing it by a regular lattice with lattice constant  $\ell_0$ . We define  $c_x^\alpha$  to be the population of genotype  $\alpha$  at the lattice point  $x$ . We then have to solve the eigenvalue equation

$$\begin{aligned} \frac{dc_x^\alpha(t)}{dt} &= \sum_{x',\alpha'} \mathcal{L}(x,\alpha,x',\alpha') c_{x'}^{\alpha'}(t) \\ &= \Gamma c_x^\alpha(t). \end{aligned} \quad (44)$$

The discretized version of the Liouville operator is

$$\begin{aligned} \mathcal{L} &= \frac{D}{\ell_0^2} \sum_x \sum_{\alpha=1}^2 \left[ e^{-\frac{v\ell_0}{2D}} |x\rangle^{\alpha\alpha} \langle x + \ell_0| \right. \\ &\quad \left. + e^{\frac{v\ell_0}{2D}} |x + \ell_0\rangle^{\alpha\alpha} \langle x| - 2 \cosh\left(\frac{v\ell_0}{2D}\right) |x\rangle^{\alpha\alpha} \langle x| \right] \\ &\quad + \sum_x [U_1(x)|x\rangle^{11} \langle x| + U_2(x)|x\rangle^{22} \langle x| \\ &\quad + \mu_1 \alpha_1 |x\rangle^{12} \langle x| + \mu_2 \alpha_2 |x\rangle^{21} \langle x|], \end{aligned} \quad (45)$$

where we have used the notation  $|x\rangle^{\alpha\beta} \langle y|$  to mean the tensor product of localized states corresponding to  $c_x^\alpha$  and  $c_y^\beta$ . We define  $U_1(x) = (a_1 - \mu_1 \alpha_1) \theta(W/2 - |x|) + (b_1 - \mu_1 \alpha_1) \theta(|x| - W/2)$ , and  $U_2(x) = (a_2 - \mu_2 \alpha_2) \theta(W/2 - |x|) + (b_2 - \mu_2 \alpha_2) \theta(|x| - W/2)$ . We impose a finite size on the system  $L$  (with periodic boundary conditions) and a finite width of the oasis  $W$ , with  $W \ll L$ .

In order for the lattice approximation to be valid, the lattice must be fine enough that variations in the eigenfunction  $\phi$  between lattice points is small. This means we must require  $\frac{\ell_0 |\partial_x \phi_n^{R,\alpha}(x)|}{\phi_n^{R,\alpha}(x)} \ll 1$ . For small  $v$  this reduces to  $\kappa_\alpha^n \ell_0 \ll 1$ ,  $k_\alpha^n \ell_0 \ll 1$ , and for large  $v$  we need  $\frac{v\ell_0}{2D} \ll 1$  (Dahmen et al., 2002). These conditions are satisfied for all of the calculations discussed here.

It is now straightforward to numerically solve for the eigenvalues and eigenstates of the lattice version of the Liouville operator  $\mathcal{L}$ . The results quoted here all use a system size  $L = 512\ell_0$ , with an oasis width  $W = 10\ell_0$  and periodic boundary conditions.

In comparing results, it is useful to shift to dimensionless units. We define a dimensionless velocity

$$\bar{v} = \frac{v}{2\sqrt{a_1 D}}. \quad (46)$$

Note that for  $\mu_1 = \mu_2 = 0$ , the extinction velocity  $\bar{v}_e = 1$ . We then scale all the growth rates to  $a_1$  by defining

$$\begin{aligned} \bar{a}_1 &= \frac{a_1}{a_1} = 1, & \bar{b}_1 &= \frac{b_1}{a_1}, & \bar{a}_2 &= \frac{a_2}{a_1}, \\ \bar{b}_2 &= \frac{b_2}{a_1}, & \bar{\alpha}_1 &= \frac{\alpha_1}{a_1}, & \bar{\alpha}_2 &= \frac{\alpha_2}{a_1}, & \bar{\Gamma} &= \frac{\Gamma}{a_1}. \end{aligned} \quad (47)$$

This implies that the dimensionless diffusion coefficient is

$$\bar{D} = \frac{1}{4}. \quad (48)$$

The mutation rates are already dimensionless. We use these redefined units in Figs. 2–4.

### Appendix D. Discrete simulation

Here we describe the details of the discrete, individual-based simulations. We begin with a discretized spatial lattice containing a uniform distribution of individuals of both types. We also discretize time, dividing it into small intervals of size  $\Delta t$ . At each time, we select a lattice point at random. The individuals at this point can give birth, move due to diffusion or drift, or mutate with appropriate probabilities. The probabilities used are simply the coefficients of the off-diagonal elements of the discretized Liouville operator described in Appendix C, times  $\Delta t$ . We set  $\Delta t$  to be sufficiently small that the probability of two or more events per step is negligible. We impose a saturation effect (analogous to a nonlinear term in Eq. (4)) by setting a maximum number of individuals per spatial point.

For the simulations described in Fig. 4, we use the parameters  $\bar{a}_1 = \bar{\alpha}_1 = 1$ ,  $\bar{a}_2 = \bar{\alpha}_2 = 0.6$ ,  $\bar{b}_1 = -1$ ,  $\bar{b}_2 = -0.6$ , and  $\bar{D} = 0.25$ , where the overbars denote the dimensionless parameters defined in Appendix C. We use a lattice with 512 points, with an oasis of width 10 points and periodic boundary conditions, and a maximum of 200 individuals per point.

For these parameter values,  $v_s$  is impossible to determine because the populations are extinct at such high velocities. However, we can determine  $v_e$  as a function of  $\mu_1$  and  $\mu_2$ . For each value of  $\mu_1$  and  $\mu_2$  that we test, we plot the total number of individuals in the steady state distribution as a function of  $v$ . This exhibits a transition from some maximum number of individuals for small  $v$  to approximately 0 individuals for large  $v$ . Because of the imposed saturation effect, the transition is not perfectly sharp but rather has some small width. We define the transition to occur at the point at which the number of individuals has dropped to  $\frac{1}{10}$  th number for  $v = 0$ . Making a different definition would shift the extinction velocities slightly.

We have also run simulations for parameter values where  $v_s$  is biologically relevant. From the  $v$ -dependence of the ratio of the number of individuals of type 1 to type 2, we can determine the value of  $v_s$  in these cases. Although the presence of saturation broadens the transition as in the case of  $v_e$ , the results match our analytical predictions.

## References

- Altmeyer, S., McCaskill, J.S., 2001. Error threshold for spatially resolved evolution in the quasispecies model. *Phys. Rev. Lett.* 86, 5819–5822.
- Burger, R., Lynch, M., 1995. Evolution and extinction in a changing environment: a quantitative-genetic analysis. *Evolution* 49, 151–163.
- Cardy, J., Tauber, U., 1996. Theory of branching and annihilating random walks. *Phys. Rev. Lett.* 77, 4780–4783.
- Dahmen, K.A., Nelson, D.R., Shnerb, N., 2002. Life and death near a windy oasis. *J. Math. Biol.* 41, 1–23.
- Doi, M., 1976a. Second quantization representation for classical many-particle system. *J. Phys. A* 9, 1465–1478.
- Doi, M., 1976b. Stochastic theory of diffusion-controlled reaction. *J. Phys. A* 9, 1479–1495.
- Endler, J.A., 1973. Gene flow and population differentiation. *Science* 179, 243–250.
- Eigen, M., 1971. Self-organization of matter and evolution of biological macromolecules. *Naturwissenschaften* 58, 465.
- Eigen, M., McCaskill, J.S., Schuster, P., 1989. The molecular quasispecies. *Adv. Chem. Phys.* 75, 149–263.
- Felsenstein, J., 1975. Genetic drift in clines which are maintained by migration and natural selection. *Genetics* 81, 191–207.
- Fisher, R.A., 1937. The wave of advance of an advantageous gene. *Ann. Eugenetic.* 7, 355–369.
- Fisher, R.A., 1950. Gene frequencies in a cline determined by selection and diffusion. *Biometrics* 6, 353–361.
- Gerland, U., Hwa, T., 2002. On the selection and evolution of regulatory DNA motifs. *J. Mol. Evol.* 55, 386–400.
- Haldane, J.B.S., 1948. The theory of a cline. *J. Genet.* 48, 277–284.
- Hanson, W.D., 1966. Effects of partial isolation (distance), migration, and differential fitness requirements among environmental pockets upon steady state gene frequencies. *Biometrics* 22, 453–468.
- Hatano, N., Nelson, D.R., 1997. Vortex pinning and non-Hermitian quantum mechanics. *Phys. Rev. B* 56, 8651–8673.
- Hatano, N., Nelson, D.R., 1998. Non-Hermitian delocalization and eigenfunctions. *Phys. Rev. B* 58, 8384–8390.
- Kamp, C., Bornholdt, S., 2002. Coevolution of quasispecies: B-cell mutation rates maximize viral error catastrophes. *Phys. Rev. Lett.* 88, 068104.
- Landau, L.D., Lifshitz, E.M., 1991. *Quantum Mechanics (Non-Relativistic Theory)*. Pergamon Press, New York.
- May, R., Endler, J.A., McMurtrie, R.E., 1975. Gene frequency clines in the presence of selection opposed by gene flow. *Am. Nat.* 109, 659–676.
- McCaskill, J.S., 1984. A localization threshold for macromolecular quasispecies from continuously distributed replication rates. *J. Chem. Phys.* 80, 5194–5202.
- Nagylaki, T., 1975. Conditions for the existence of clines. *Genetics* 80, 595–715.
- Nagylaki, T., 1978. Clines with asymmetric migration. *Genetics* 88, 813–827.
- Neicu, T., Pradhan, A., Larochelle, D.A., Kudrolli, A., 2000. Extinction transition in bacterial colonies under forced convection. *Phys. Rev. E* 62, 1059–1062.
- Nelson, D.R., Shnerb, N., 1998. Non-Hermitian localization and population biology. *Phys. Rev. E* 58, 1383–1403.
- Nilsson, M., Snoad, N., 2000. Error thresholds for quasispecies on dynamic fitness landscapes. *Phys. Rev. Lett.* 84, 191–194.
- Nilsson, M., Snoad, N., 2002. Optimal mutation rates in dynamic environments. *Bull. Math. Biol.* 64, 1033–1043.
- Pauwelussen, J.P., Peletier, L.A., 1981. Clines in the presence of asymmetric migration. *J. Math. Biol.* 11, 207–233.
- Peliti, L., 1985. Path integral approach to birth-death processes on a lattice. *J. Phys.* 56, 1469–1483.
- Roughgarden, J., 1974. Population dynamics in a spatially varying environment: how population size “tracks” spatial variation in carrying capacity. *Am. Nat.* 108, 649–664.
- Slatkin, M., 1973. Gene flow and selection in a cline. *Genetics* 75, 733–756.
- Slatkin, M., Maruyama, T., 1975. Genetic drift in a cline. *Genetics* 81, 209–222.
- Wiens, J., 1976. Population responses to patchy environments. *Ann. Rev. Ecol. Systems* 7, 81–120.
- Wilke, C., Ronnewinkel, C., 2001. Dynamic fitness landscapes: expansions for small mutation rates. *Physica A* 290, 475–490.
- Wilke, C., Ronnewinkel, C., Martinetz, T., 2001. Dynamic fitness landscapes in molecular evolution. *Phys. Rep.* 349, 395–446.
- You, L., Nagylaki, T., 2002. A semilinear parabolic system for migration and selection in population genetics. *J. Differential Equations* 181, 388–418.